Histol Histopathol (2011) 26: 1435-1452

http://www.hh.um.es

Histology and Histopathology

Cellular and Molecular Biology

Alterations of the perivascular dystrophin-dystroglycan complex following brain lesions. An immunohistochemical study in rats

M. Kálmán, J. Mahalek, A. Adorján[1], I. Adorján, K. Pócsai, Z. Bagyura[2] and S. Sadeghian

Deptartment of Anatomy, Histology and Embryology, Semmelweis University, Budapest, Hungary

[1]Present address: Dept. of Anatomy, Szent István University, Budapest

[2]Present address: Heart Center, Semmelweis University, Budapest

Summary. Dystroglycan is a laminin receptor, which with dystrophins and other components forms the dystrophin-dystroglycan complex. It has an important role in the formation of gliovascular connections, cerebral vascularisation and blood-brain barrier. Dystroglycan consists of two sub-units, α and ß. Previous studies demonstrated that the ß-dystroglycan immunoreactivity of cerebral vessels temporarily disappeared in the area adjacent to the lesion, whereas the vascular laminin which is not immunoreactive in the intact brain became detectable. The present study extends these investigations over other components of the complex: utrophin, α1-syntrophin and α1-dystrobrevin. The experiments were performed on adult rats. The lesions were stab wounds or cryogenic lesions in deep ketamine-xylasine narcosis. Following survival periods 2 to 30 days, the animals were perfused and floating brain sections were processed for fluorescent immunohistochemistry. The α1-dystrobrevin, like ß-dystroglycan, vanished temporarily around the lesion. The immunoreactivity of utrophin changed in a similar way to that of laminin. In intact brains they were confined to the entering segments of the vessels and to the circumventricular organs. Following lesions their immunoreactivity manifested in the vessels around the lesions. However, utrophin followed laminin with a delay: their peaks were about POD (postoperative days) 21 and 7, respectively. Only immunoreactivity of α1-syntrophin appeared in the reactive astrocytes, peaking at POD 14. Double-labeling proved its co-localization with GFAP. Cryogenic lesions had similar immunohistochemical effects, but provided more suitable samples for Western blot analysis, which proved the altered levels of α1-dystrobrevin and α1-syntrophin. The phenomena may help to monitor the *post-lesion* vascular processes and the alterations of the gliovascular connections.

Key words: Cerebrovascular basal lamina, Dystrobrevin, Laminin, Syntrophin, Utrophin

Offprint requests to: M. Kálmán, Dept. of Anatomy, Histology and Embryology, Semmelweis University, M-1094, Tuzolto 58, Budapest, Hungary. e-mail: kalman@ana.sote.hu

Introduction

Dystroglycan binds laminin and other basal lamina components (e.g. perlecan and agrin: Henry and Campbell, 1996a,b). Similarly to dystrophin, dystroglycan was at first described in the skeletal muscle but later also in other tissues, including the brain (for early reviews, see Henry and Campbell, 1996a; Durbeej et al., 1998). Dystroglycan associates with dystrophins and several other components to form the dystrophin-dystroglycan complex (or dystrophin-glycoprotein complex, DGC). DGC integrates aquaporin water-channels, ion-channels and signalling systems, as well as the actin filament system to the part of the cell membrane where it contacts the basal lamina (Guadagno and Moukhles, 2004; Wolburg et al., 2009). It plays an important role in the formation of muscles, blood vessels and parenchymal organs, such as kidney and lung (Haenggi and Fritschy, 2006). Its significance in the brain has also been demonstrated (see e.g. Blake et al., 1999; Culligan and Ohlendieck, 2002; Amiry-Moghaddam et al., 2004; Haenggi and Fritschy, 2006; Wolburg et al., 2009).

Laminin is a ubiquitous major component of the basal laminae, therefore it has been proved to be essential for brain vascularization and *post-lesion* rearrangement of vessels (for review, see e.g. Hallmann

et al., 2005). The receptors of laminin therefore are also essential in vascularisation.

In the brain, integrity of the DGC as well as the binding of laminin to dystroglycan is required for gliovascular coupling, maturation and stabilization of the cerebral vascular structure (Tian et al., 1996; Zaccaria et al., 2001; Nico et al., 2003, 2004; del Zoppo et al., 2006). The gliovascular connections are necessary for the endothelial cells to form blood-brain barrier (Janzer and Raff, 1987; Tao-Cheng et al., 1987; Riseau and Wolburg, 1990; Abbott, 2002). Deletion of dystroglycan in mice results in discontinuity of the cerebrovascular basal laminae (Moore et al., 2002).

Dystroglycan is encoded by a single gene and cleaved by post-translational processing into two proteins: α- and ß-dystroglycan (Ibraghimov-Beskrovnaya et al., 1992; Smalheiser and Kim, 1995). ß-dystroglycan is a highly glycosylated extracellular protein which binds laminin and other basal lamina components, e.g. agrin, perlecan. ß-dystroglycan is a transmembrane protein that anchors α-dystroglycan to the cell membrane.

ß-dystroglycan, as the core component of DGC, interacts at its intracellular side with different dystrophin/utrophin isoforms. Dystrophin, or, alternatively, utrophin, its autosomal homologue binds dystrobrevins (α1, α2 or ß), syntrophins (α1,α2, ß, γ1 or γ2) and actin filaments, connecting these components to the ß-dystroglycan. (For more detailed descriptions, see e.g. Ueda et al., 1995; Culligan and Ohlendieck, 2002; Amiry-Moghaddam et al., 2004; Warth et al., 2004; Wolburg et al., 2009)

Even in the brain the composition of DGC depends on its localization. In the perivascular glial end-feet α1-dystrobrevin, α1-syntrophin and the 71kD dystrophin isoform are found (Culligan and Ohlendieck, 2002; Haenggi and Fritschy, 2006; Wolburg et al., 2009). Dystrophin isoforms, shorter protein products of the dystrophin gene, which arise by alternative promoter usage, are found in various tissues. In the brain, the Dp71 isoform is localized mainly in glial cells, while the full-length form, Dp427, is found mainly in neurons, primarily in the postsynaptic densities (see e.g. Gorecki et al., 1992; Lederfein et al., 1992; Lidov, 1996; Haenggi and Fritschy, 2006). In contrast to the glial end-feet, in the endothelial cells utrophin occurs, and dystroglycan is supposed to be missing (Haenggi and Fritschy, 2006). Sarcoglycan and sarcospan, intramembrane components of DGC in muscle, very probably are lacking in the brain (Culligan and Ohlendieck, 2002).

The complex, first of all its syntrophin component, is responsible for the proper distribution and anchoring of ion channels and receptors, including the water-pore channel protein, aquaporin-4 along the plasma membrane. α1-syntrophin and α1-dystrobrevin connect sodium-channels, Grb2 and nitric oxide-synthase (NOS) systems (Neely et al., 2001; Amiry-Moghaddam et al., 2004; Warth et al., 2004; Wolburg et al., 2009).

Astroglia are involved in these phenomena for several reasons. The importance of the gliovascular connections, and the glial localization of DGC have been mentioned above. Astrocytes produce laminin and other components of basal lamina (Liesi et al., 1984; Bernstein et al., 1985; Chiu et al., 1991; Jucker et al., 1996). Brain lesions are followed by astroglial reaction. Astrocytes have a decisive role in *post-lesion* vessel formation (Krum et al., 2002).

In previous studies the ß-dystroglycan immunoreactivity of brain vessels weakened considerably following lesions, including focal ischemia (Milner et al., 2008), experimental autoimmune encephalomyelitis (Agrawal et al., 2006), or the area of stab wounds (Szabó and Kálmán, 2008). Laminin immunoreactivity, on the other hand, which was confined to the entering segments of vessels in the intact brain, became visible in vessels around lesions (Sosale et al., 1988; Shigematsu et al., 1989 a,b; Krum et al., 1991; Sixt et al., 2001; Szabó and Kálmán, 2004, 2008). Dystrophins were studied by Jancsik and Hajós (1998, 1999), and Szabó et al. (2004) during development and following lesions.

The present study extended the previous investigations in two directions. We have undertaken to follow the *post-lesion* changes of three additional DGC components by immunohistochemistry: utrophin, α1-syntrophin, and α1-dystrobrevin. Furthermore, in addition to stab wounds we applied cryogenic lesions as well. We have found that in contrast to the stab wounds, the shape and size of the lesioned territories were fairly uniform in the case of the cryogenic lesions. This enabled us to assess the changes of protein levels by Western blot analysis. The immunoreactivity results demonstrated that the *post-lesion* phenomena of DGC were fundamentally concordant in the case of these two lesion types. *Post-lesion* glial reaction was monitored by immunohistochemical staining of GFAP (glial fibrillary acidic protein), the characteristic intermediate filament protein of mature astrocytes which increases considerably in the reactive glia (Bignami and Dahl, 1976; Berry et al., 1983; Mathewson and Berry, 1984; Hozumi et al., 1990). Postoperative survival times were calculated from these results, and from our previous studies (Szabó and Kálmán, 2004, 2008).

Materials and methods

Animals

Adult rats (Wistar) of either sex weighing 250 to 300 g were used. The animals were supplied with food and water *ad libitum*, and kept in artificial 12/12 h light-and-dark periods. All experimental procedures were performed in accordance with the guidelines of European Community Council Directive (86/609/EEC).

Stab wounds

Adult albino rats of either sex were anesthetized deeply with ketamine and xylazine (20 and 80 mg/kg body weight, respectively, intramuscularly). After opening the skin and making a burr hole on the skull, a

lesion was performed on the dorsal side of the parietal cortex with a sterile disposable needle, then the skin was sutured and the animals were allowed to recover. The survival period lasted for 2, 4, 7, 14, 21, or 28, postoperative days (POD; 3 to 4 animals at each).

Cryogenic lesions

Anaesthesia was the same as before. The skin was opened and a bone piece was removed by drilling, so a 'window' was formed on the skull. The lesion was performed on the dorsal side of the parietal cortex by a 20-sec contact of a copper rod adjusted to a stereotaxic instrument and cooled in carbondioxyde 'snow'. Then the bone piece was repositioned and the skin sutured. Survival periods were as before.

Fixation and sectioning

Anaesthesia was the same as before. The animals were perfused through the aorta with 100ml 0.9% sodium chloride followed by 300 ml 4% para-formaldehyde in 0.1M phosphate buffer (pH 7.4). After perfusion brains were removed and post-fixed in the same fixative for 1-2 days at 4°C. Then serial coronal sections of 50 μm were cut with Vibratome through the lesioned area, and washed in phosphate buffered-saline 0.1 M, pH 7.4 (PBS, Sigma) overnight.

Immunohistochemistry

Primary immunoreagents are listed in Table 1. Floating sections were pretreated with normal goat serum (horse serum in the case of anti-α-dystrobrevin), diluted to 20% in PBS for 90 min to block the non-specific binding of antibodies. This and the following steps were followed by an extensive wash in PBS (30 min, at room temperature). Primary antibodies were diluted as described in Table 1 in PBS containing 0.5% Triton X-100 and 0.01% sodium azide. Sections were incubated for 40 h at 4°C. Fluorescent secondary antibodies (Table 2) were used at room temperature for 3 h. The sections were finally washed in PBS (1 h, at room temperature), mounted onto glass, cover-slipped in a mixture of glycerol and bi-distilled water (1:1), and sealed with lacquer. Control sections were done by substituting the primary antibody with normal serum. No structure-bound fluorescent labeling was observed in these specimens.

Intensities of fluorescent labeling were compared as follows: the sensitivity of the digital camera was turned down until the immunolabeling was not detectable on the display, and the degree of turning down was estimated by the arbitrary units of sensitivity marked by the manufacturer. In this way the immunoreactivities of the same substance were compared at different postoperative days. Differences between substances we did not compare, since they also depended on the different intensities of the immunobindings and fluorophore labelings of the secondary antibodies beside the immunoreactivities of the epitopes investigated.

Double-labeling immunofluorescent reactions

Double-labeling experiments were performed where antibodies of different origin (e.g. mouse *versus* rabbit) were available against the different components. The corresponding primary and secondary antibodies were applied together, otherwise the protocol was the same as before.

Confocal laser scanning microscopy and digital imaging

Slides were photographed by a DP50 digital camera mounted on an Olympus BX-51 microscope (both from Olympus Optical Co. Ltd, Tokyo, Japan), or, in the case of double labelings, by a Radiance-2100 (BioRad, Hercules, CA) confocal laser scanning microscope. Digital images were processed using Photoshop 9.2 software (Adobe Systems, Mountain View, CA) with minimal adjustments for brightness and contrast. Green and red colors on the photomicrographs correspond to the fluorescent dyes as shown in Table 2.

Western blot

Lesioned tissue samples were obtained from 6 animals with cryogenic lesion on the dorsal side of the parietal cortex. Similar tissue pieces from 3 intact cortices served as controls. Tissue samples were immediately frozen in liquid nitrogen and stored at -80°C until lysis. Cell lysates were obtained by using the following buffer: 150 mM sodium chloride, 1.0% NP-40, 0.5% sodium deoxycholate, 0.1% sodium dodecyl

Table 1. The primary antibodies applied in the sudy.

Against	Type	Firm	Code Nr.	Dilution
ß-dystroglycan	Mouse*	Novocastra, Newcastle-on-Tyne, England	ncl-b-dg	1:100
α-dystrobrevin	Goat**	Santa Cruz Biotechnology, Santa Cruz, Ca, USA	(v-19) sc-13812	1:100
α1-syntrophin	Rabbit**	Sigma, San Louis, Mo, USA	s4688	1:100
utrophin	Mouse*	Novocastra, Newcastle-on-Tyne, England	ncl-drp2	1:10
GFAP	Mouse*	Novocastra, Newcastle, United Kingdom	ga5	1:100
EHS Laminin	Rabbit**	Sigma, San Louis, Mo, USA	l 9393	1:100

*: monoclonal; **: polyclonal

sulphate (SDS) in 50 mM Tris, pH 8.0. Proteolysis was blocked with protease inhibitor cocktail (Sigma P8340). Samples were first homogenized in the above buffer at 4°C, then the homogenate was centrifuged. Protein contents were determined by the method of Lowry et al. (1951), with bovine serum albumin (BSA) as standard. Electrophoresis of cell lysates (10 μg per channel) was carried out in 7.5% SDS polyacrylamid gels as described by Laemmli (1970). Proteins were then transferred electrophoretically to PVDF membrane (Millipore Immobilon-P transfer membrane) and blocked with 5% non-fat dried milk in TPBS (PBS with 0.3 % Tween 20). Proteins were probed with primary antibodies recognizing α1-dystrobrevin and α1-syntrophin. Peroxidase conjugated anti-goat, anti-rabbit or anti-mouse IgGs (Vector Laboratories) were used as secondary antibodies, respectively. Visualization was performed by using Supersignal West Pico Chemiluminescent Substrate (Pierce 34080). Chemiluminescent signal detection was by exposure to Amersham Hyperfilm ECL (28-9068-35).

Semiquantitative data were obtained by analysing the scanned films with the "gel analysis" option of ImageJ program. Numerical data obtained by integrated density measurements were used. Data obtained from the lesioned tissue were compared with the control.

Results

Laminin and DGC component immunoreactivities in the intact adult rat brain (Fig. 1)

Laminin was detectable in the meningeal tissue and vessels, but not throughout the brain, only in the segments of the vessels where they enter the brain, corresponding to the Virchow-Robin spaces (Fig. 1a), as well as in the circumventricular organs (subfornical organ (Fig. 1b), median eminence, area postrema, but not the subcommissural organ). Neurons were also labeled, mainly in the cortex and in the hippocampus.

The distribution of utrophin immunoreactivity was similar to that of laminin: the meninges, their vessels including the segments where they enter the brain substance (Fig. 1c), and circumventricular organs were reactive (Fig. 1d), but not the cerebral vessels in general. Immunostaining of αl-syntrophin marked the meningeal surface and the entering vessels, marked scarcely the deeper vessels of the brain substance, and neurons only faintly (Fig 1e).

The ß-dystroglycan immunostaining revealed a rich vascular system in every part of the brain (Fig. 1f). A ß-dystroglycan-immunopositive layer lined the meningeal surface as well, whereas the meningeal vessels remained immunonegative. Brain vessels were also visualized completely by immunohistochemical reaction to α1-dystrobrevin (Fig. 1g), like in the case of ß-dystroglycan, but less intensively stained. No astrocytic profiles were immunoreactive to either component investigated in the intact brain.

Laminin and ß-dystroglycan immunoreactivities following stab wounds: opposite (anti-coincident) localizations (Fig. 2)

Following stab wounds, by POD 2 the adjacent vessels lost their ß-dystroglycan immunopositvity, whereas immunopositivity to laminin became detectable in them. When laminin and ß-dystroglycan immunostainings were combined (Fig. 2a-d), vascular laminin immunopositivity was confined to the site of the lesion and was found usually in vessels not labeled by immunoreaction against ß-dystroglycan. In the surrounding area, some distance from the lesion, the vessels proved to be immunoreactive only to ß-dystroglycan, although at the border of the two zones double-labeled vessels also occurred. In neurons laminin immunopositivity sometimes occurred, like in the intact tissue. After the third postoperative week laminin immunopositivity regressed to the close vicinity of the lesion or disappeared, whereas ß-dystroglycan immunoreactivity covered the whole territory of the lesion (Fig. 2e,f), so the rest of the laminin-immunoreactive vessels became dystroglycan immunopositive as well. Astrocytes displayed no immunoreactivity to either ß-dystroglycan or laminin.

α1-dystrobrevin and ß-dystroglycan immunoreactivities following stab wounds: parallel temporary vanishing (Fig. 3)

α1-dystrobrevin immunoreactivity, which delineated the vessel system in intact animals, disappeared from the vessels adjacent to the lesion (Fig. 3a,b), by POD 2, similarly to ß-dystroglycan. The phenomenon was even

Table 2. The secondary antibodies applied in the study.

Conjugated with	Against	Type	Absorbead light / Emitted light (nm)	Firm	Code Nr.	Dilution
Fluorescein isothio-cyanate (FITC)	Rabbit	Donkey	492 (blue) / 520 (green)	Jackson Immunoresearch Laboratories, West Grove, Pa, USA	711-095-152	1:250
Fluorescein isothio-cyanate (FITC)	Goat	Donkey	492 (blue) / 520 (green)	Jackson Immunoresearch Laboratories, West Grove, Pa, USA	705-093-003	1:250
Cy3	Mouse	Donkey	550 (green) / 570 (red)	Jackson Immunoresearch Laboratories, West Grove, Pa, USA	715-165-150	1:250

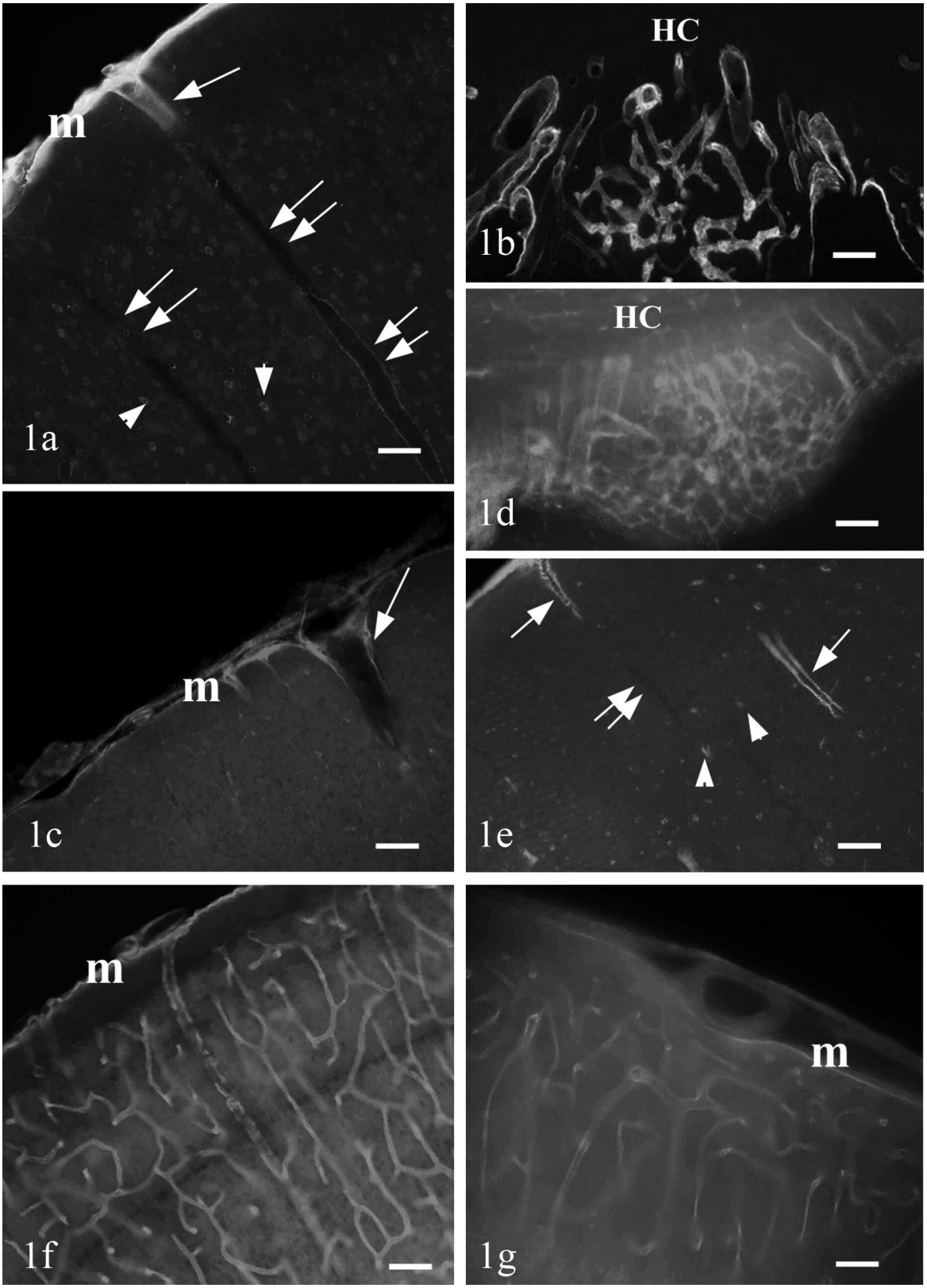

Fig 1. Laminin and DGC component immunoreactivities in the intact adult rat brain. **a.** Laminin immunostaining decorates only the meningeal surface (m) and the segments (arrow) of vessels entering the brain. Note the unlabeled but visible continuing part of the vessel in the brain substance (double arrows). Immunoreactivity of varied intensity can be found in neurons (arrowheads). **b.** Laminin immunostaining also visualizes the circumventricular organs, here: the subfornical organ (HC- hippocampal commissure). **c.** Utrophin immunostaining. As in the case of laminin, the meningeal surface (m) and the segments of the vessels (arrows) entering the brain are labeled. **d.** Utrophin immunoreactivity is also detectable in the circumventricular organs, here in the subfornical organ (HC- hippocampal commissure). **e.** α1-syntrophin immunostaining: only the meningeal surface and some vessels (arrows) are labeled, as well as neurons (arrowheads), other vessels are not labeled (double arrows). **f.** ß-dystroglycan immunostaining visualizes the brain vasculature as well as the meningeal surface (m), whereas meningeal vessels remain invisible. **g.** α1-dystrobrevin immunostaining results in a pattern similar to that of ß-dystroglycan, m: meningeal surface. Scale bar: a, c-g, 100 μm; b, 50 μm.

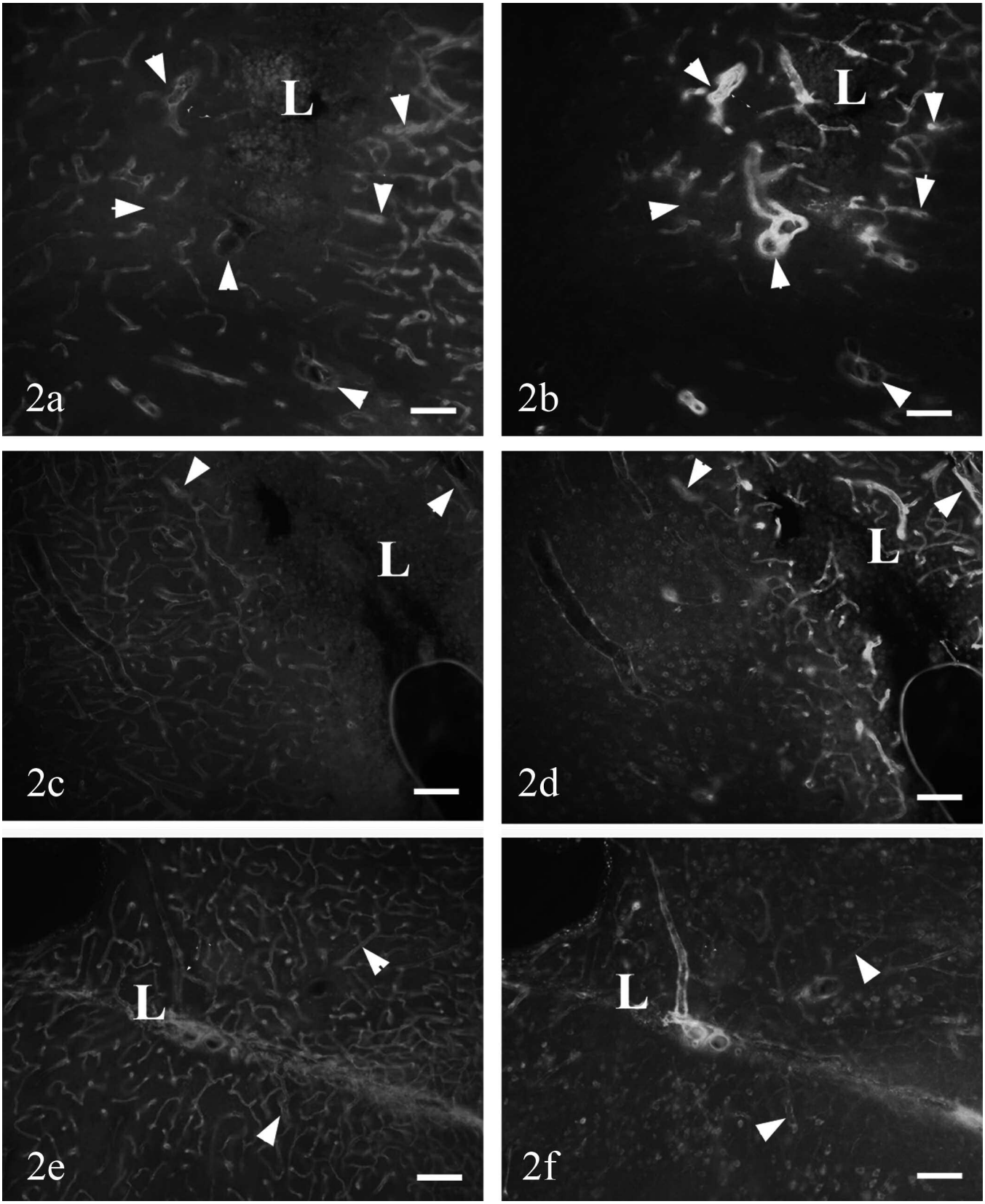

Fig. 2. Laminin and ß-dystroglycan immunoreactivities following stab wounds: opposite (anti-coincident) localizations. **a and b.** ß-dystroglycan and laminin immunopositivities, respectively, in cerebral vessels following lesion (POD 2). Double-labeling study. The laminin-immunopositive vessels **(b)** are confined to the lesioned area (L) whereas ß-dystroglycan-immunopositive ones **(a)** are found at a distance. Arrowheads point to double-labeled vessels identical in the two panels. **c and d.** POD 7 – similar distributions of immunoreactivities as in **a and b**, respectively. Marks as above. **e and f.** POD 14 – -dystroglycan immunopositivity has appeared in the vessels adjacent to the lesion. Laminin immunopositivity has regressed. Marks as above. Scale bar: a, b, e, f, 50 μm; c, d, 100 μm.

more obvious in the later days (POD 4 or 7). It seemed that the persisting immunoreactivities of both proteins were found co-localized in the same vessels. No astrocytes were immunostained. The re-appearances of the α1-dystrobrevin and ß-dystroglycan immunoreactivities (POD 14 - POD 21) were not parallel perfectly i.e. vessels immunopositive to ß-dystroglycan but negative to α1-dystrobrevin were found (Fig. 3c,d). By the end of the observation (POD 28) all the vessels were immunopositive to both proteins, like in intact animals.

Utrophin immunoreactivity following stab wounds: follows laminin but with delay (Fig. 4)

Following stab wounds by POD 7 utrophin immunopositivity appeared in a part of the vessels which were immunopositive to laminin around the lesion, as double labeling studies demonstrated. By the end of the second week utrophin and laminin immunopositivities become matching and co-localizing (Fig. 4a,b). In the necrotic tissue hardly any utrophin immunoreactivity was detected if at all. In these areas a dense network of vessels was visualized by immunohistochemical reaction against laminin, although utrophin immunostaining marked only the largest vessels, and even in these vessels the labeling was incomplete (Fig. 4c,d).

By POD 21 the utrophin-immunopositive vessels already surpassed in number the laminin-immunopositive vessels, which were already disappearing (i.e. losing their positivity). Consequently, vessels immunopositive to utrophin but not to laminin were frequently seen (Fig. 4e,f). By POD 28 both laminin and utrophin immunoreactivities were confined to the close vicinity of

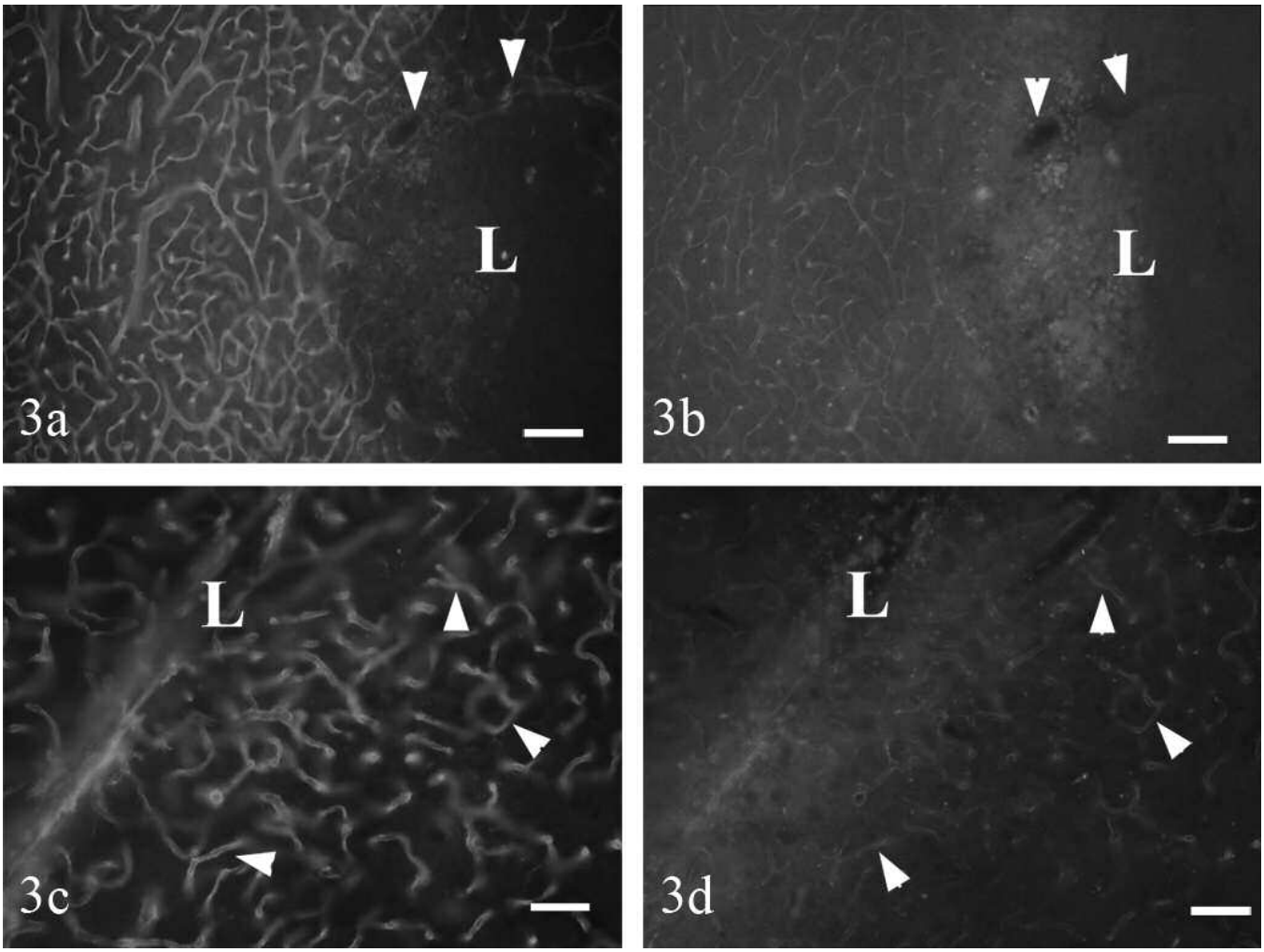

Fig. 3. α1-dystrobrevin and ß-dystroglycan immunoreactivities following stab wounds: parallel temporary vanishing. **a and b.** ß-dystroglycan and α1-dystrobrevin, respectively, in cerebral vessels following lesion (POD 7). Double-labeling study. In the zone around the lesion (L) no immunolabeled vessels are found. Note the identical patterns of the two stainings (arrowheads mark points identical in the two panels). **c and d.** A similar double-labeling at POD 14. Around the lesion (L) the vessels are immunopositive to ß-dystroglycan but negative to α1-dystrobrevin. At a greater distance the vessels are immunopositive to both (arrowheads mark points identical in the two panels). Scale bars: 50 μm.

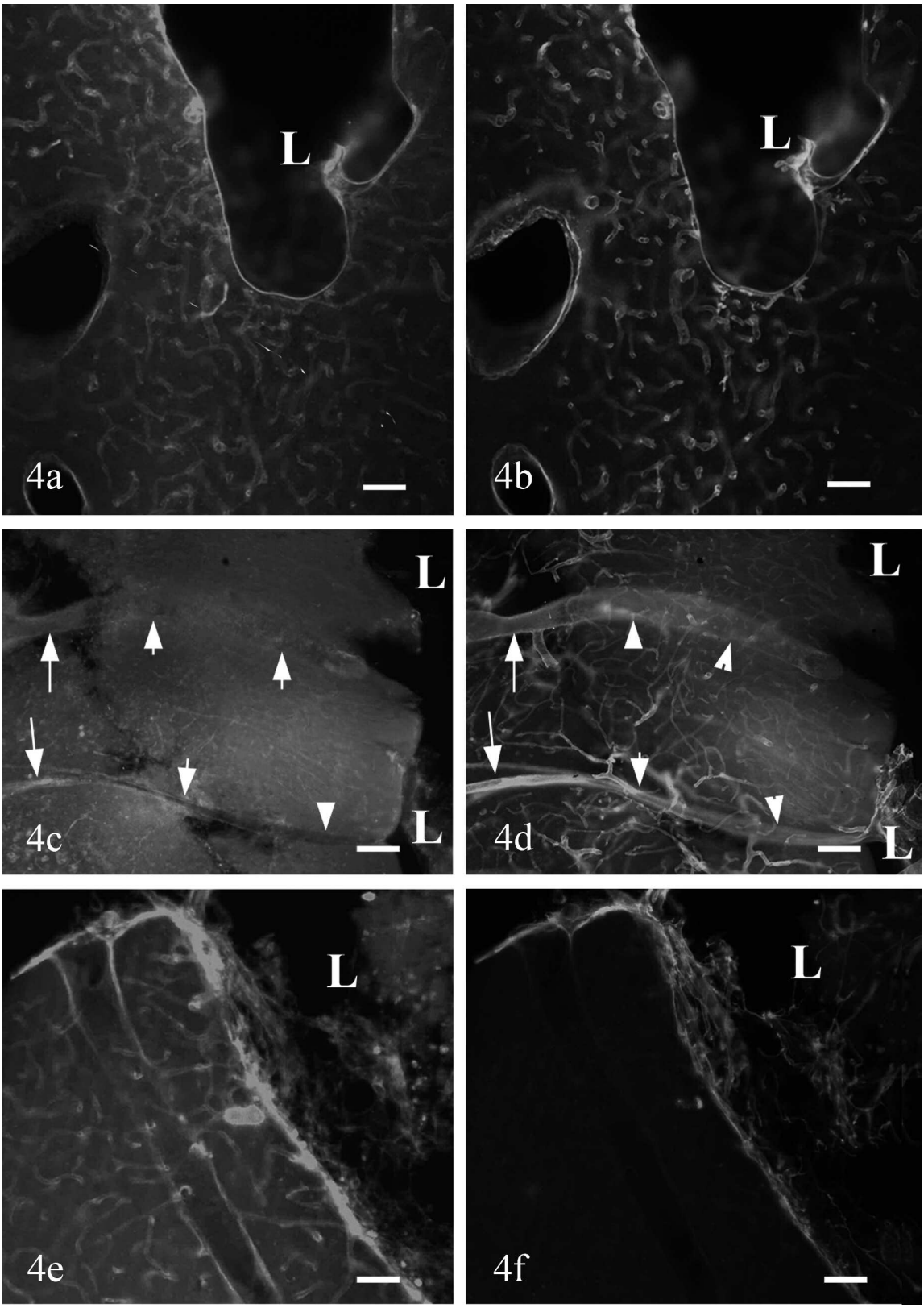

Fig. 4. Utrophin immunoreactivity following stab wounds: follows laminin but with delay. **a and b.** Utrophin and laminin immunoreactivities, respectively, in cerebral vessels following lesion, double-labeling study. At POD 14 both immunoreactivities were detectable at approximately equal intensely and co-localizing. Note the identical points in the figures (arrows). L: lesion. **c and d.** Utrophin and laminin immunoreactivities, respectively, double labeling, POD 14. In the necrotic tissue laminin immunoreactivity **(d)** visualizes a rich network of vessels (arrows mark identical points in both panels), whereas the immunoreactivity to utrophin **(c)** weakens toward (arrowheads) the necrotized tissue island. The small vessels are immunoreactive intensely to laminin, but immunonegative to utrophin. L: lesion. **e and f.** Utrophin and laminin immunoreactivities, respectively, in cerebral vessels following lesion, double labeling. At POD 21 utrophin immunoreactivity predominates **(e)**, that of laminin **(f)** has almost disappeared, numerous utrophin-immunoreactive vessels are negative to laminin. L: lesion, scale bars: 50 μm.

the lesion, if they could still be detected at all.

Utrophin and αl-dystrobrevin immunoreactivities: a final convergence (Fig. 5)

At the beginning utrophin and α1-dystrobrevin were detected in different vessel populations: the former in the distant vessels, co-localizing with the ß-dystroglycan, the latter in the vessels adjacent to the lesion site like laminin. As described above, ß-dystroglycan and laminin immunoreactivities tended later to co-localize. A similar tendency was found in the case of utrophin and α1-dystrobrevin. At POD 14 these proteins already occurred together in some vessels near the lesion (Fig. 5a,b). Later (POD 28), however, utrophin immunopositivity disappeared or almost disappeared, whereas α1-dystrobrevin immunopositivity persisted (Fig. 5c,d). Similarly to laminin and ß-dystroglycan, no utrophin labeled astrocytes were found.

α1-syntrophin imunoreactivity following stab wounds: appearance in reactive astrocytes (Fig. 6.)

Stab wounds were surrounded by an intense glial reaction, like brain lesions in general (not shown in figure). Immunostaining to α1-syntrophin marked reactive astrocytes already at POD 4 (Fig. 6a) but the maximum was found at POD 14 (Fig. 6b). Double immunolabeling demonstrated the co-localization of αl-syntrophin and the astrocyte marker GFAP (see later). The area colonized by GFAP-immunopositive astrocytes, however, surpassed what was occupied by the

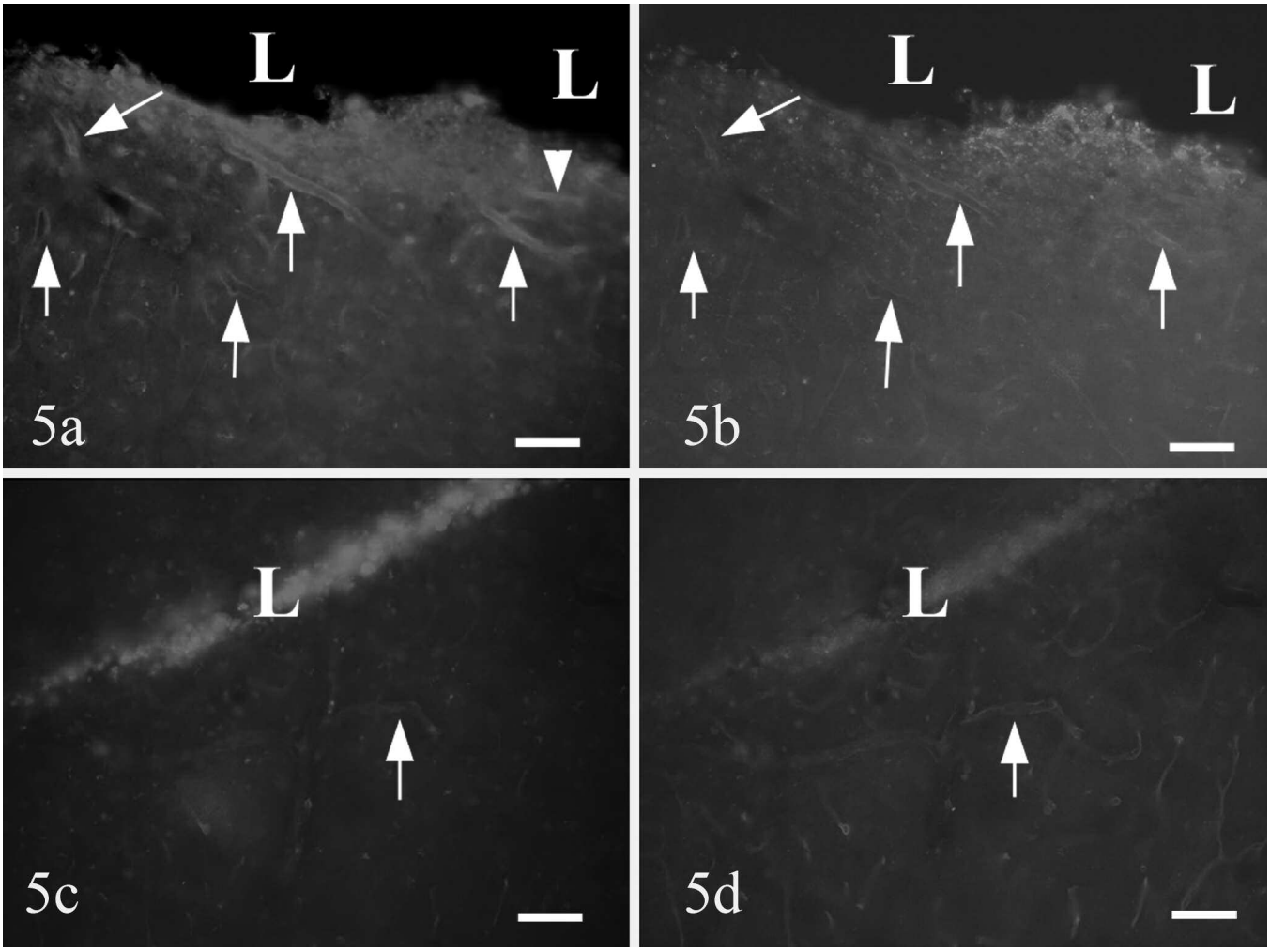

Fig. 5. Utrophin and α1-dystrobrevin immunoreactivities: a final convergence. **a and b.** Utrophin and α1-dystrobrevin immunoreactivities, respectively, in cerebral vessels following lesion, double labeling study, POD 14. α1-dystrobrevin immunopositivity **(b)** has extended to the site of the lesion (L), and appeared in the utrophin-immunopositive **(a)** vessels (arrows mark identical points in both panels). **c and d.** Utrophin and α1-dystrobrevin-immunoreactivities, respectively, in cerebral vessels following lesion, double labeling study, POD 28. The α1-dystrobrevin immunopositive vessels **(d)** are numerous around the lesion (L), whereas utrophin **(c)** has almost disappeared, arrows mark identical points in both panels. Scale bars: 50 μm.

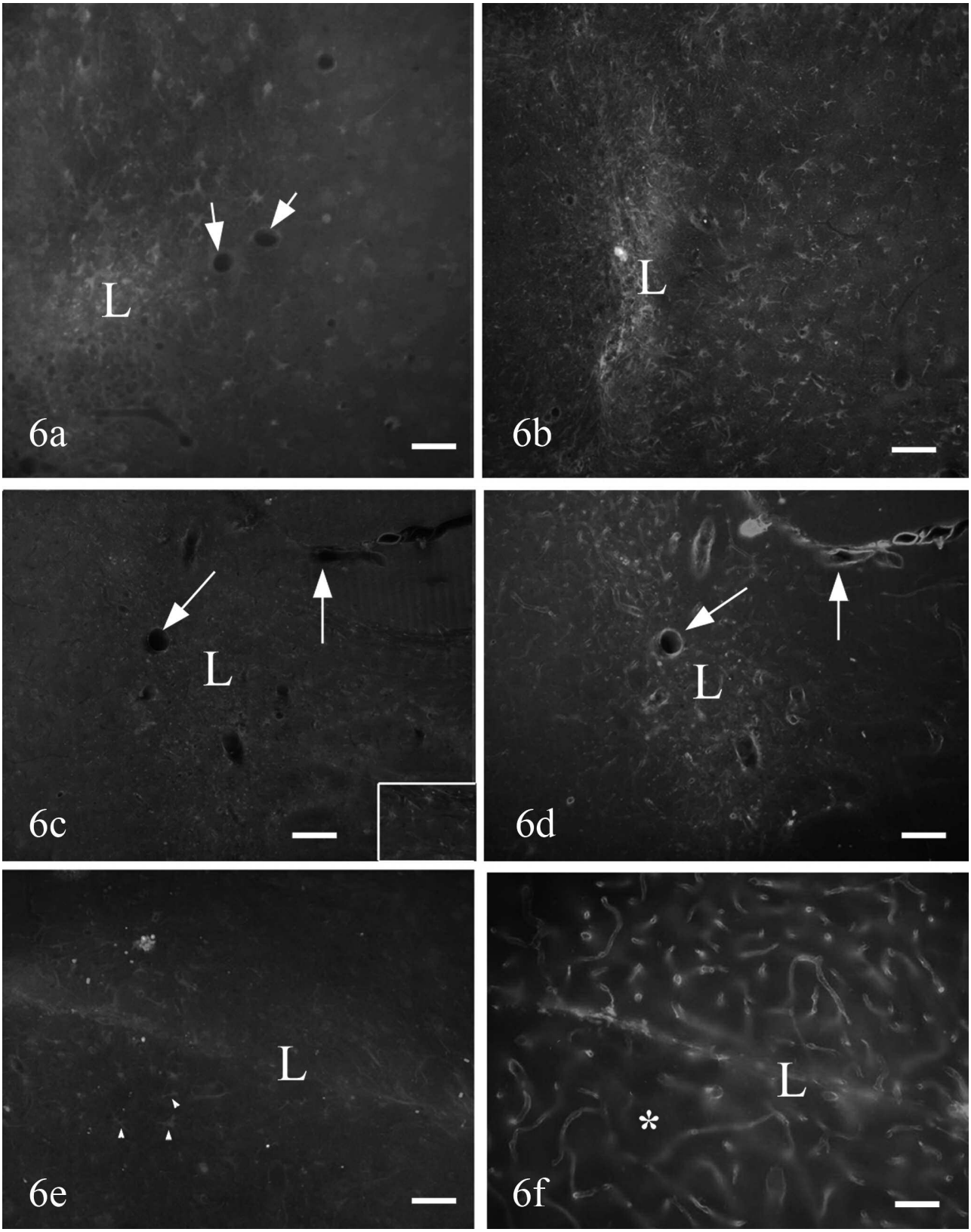

Fig. 6. α1-syntrophin imunoreactivity following stab wounds: appearance in reactive astrocytes **a and b.** α1-syntrophin immunostaining visualizes reactive astrocytes around lesions (L) already from POD 4 **(a)** but most intensely about POD 14 **(b)**. Vessels are scarcely labeled (arrows). **c and d.** α1-syntrophin and utrophin immunoreactivities, respectively, around a lesion (L), POD 28, double labeling study. Note that utrophin immmunostaining still labels vessels, whereas α1-syntrophin immunopositivity is very weak (arrows mark identical points), immunopositive astrocytes (inset) have become extremely scarce. **e and f.** α1-syntrophin and ß-dystroglycan immunoreactivities, respectively, around a lesion (L), POD 28, double labeling study. The ß-dystroglycan immunopositivity has already re-appeared even in the vessels adjacent to the site of the lesion (L). α1-syntrophin immunopositive astrocytes (arrowheads) are already confined to a resticted area. In this area (asterisk in panel **f**), however, there is no ß-dystroglycan immunostaining yet. Scale bars: 50 μm; inset in c, 25 μm.

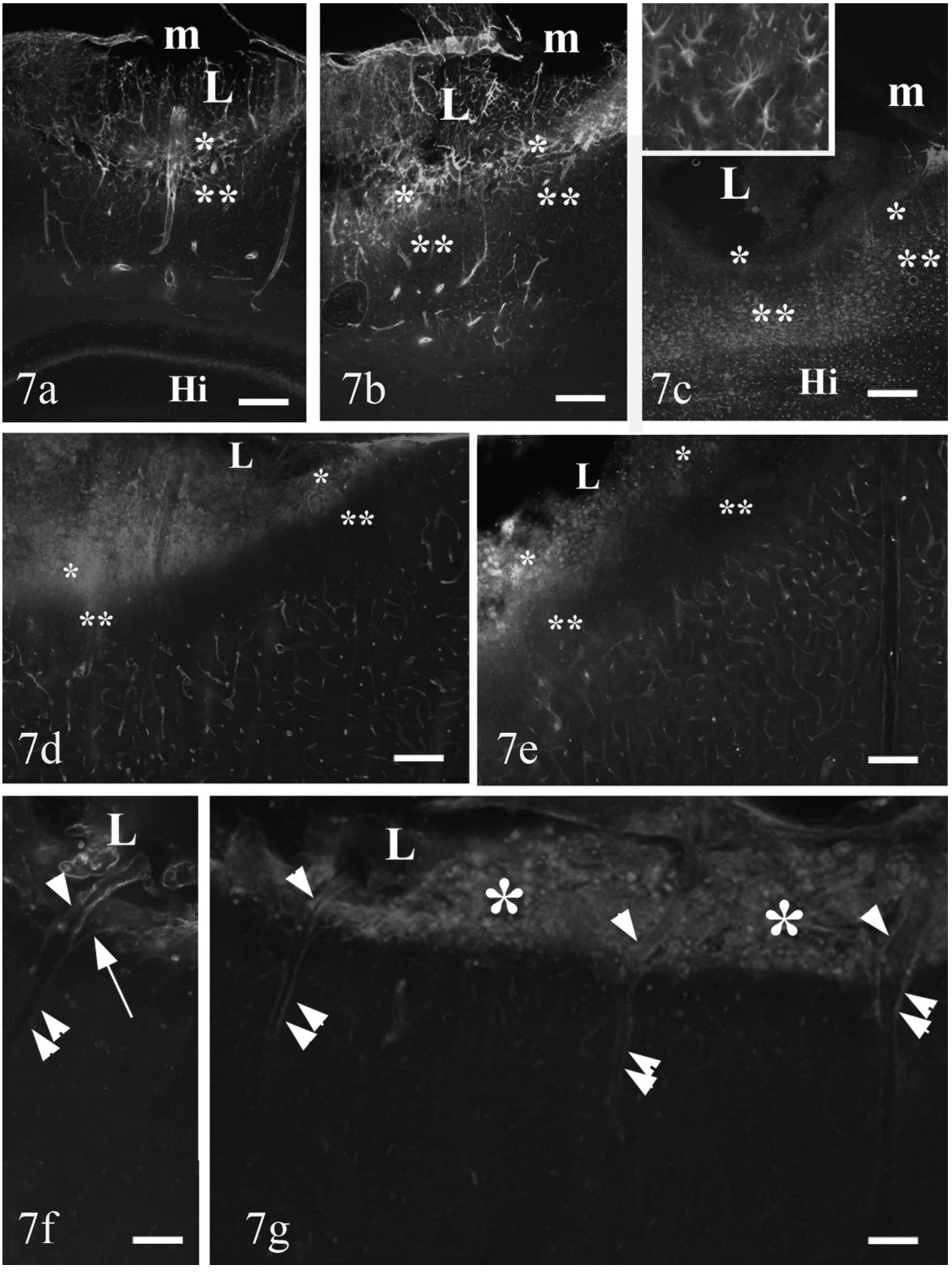

Fig. 7. Following cryogenic lesion: phenomena like above. **a.** Laminin immunostaining, a survey under low-power objective. Immunoreactivity extends in the vessels to the hippocampus (Hi). The extent of the lesion (L) and the vascular immunoreaction can be estimated. Asterisk: necrotic zone, double asterisk: zone underlying the necrotic tissue (devoid of ß-dystroglycan and α-dystrobrevin immunoreactivities, see panels **d and e**), m- meninx, Hi: hippocampus. **b.** Laminin immunostaining, higher magnification, m: meninx, asterisk: necrotic zone, in which a number of vessels (probably all of them) are immunopositive to laminin. Laminin-positive vessels penetrate the underlying zone (double asterisk, devoid of ß-dystroglycan and αl-dystrobrevin immunoreactivities, see panels **d and e** and even the tissue in which the vessels preserve their immunostaining to ß-dystroglycan and α1-dystrobrevin. **c.** GFAP immunostaining, a survey under low-power objective from a section similar to that seen in panel a). Note the intense glial reaction in the whole thickness of the cortex. L: lesion, m: meninx, Hi: hippocampus. Inset: typical astrocytes enlarged. **d.** ß-dystroglycan immunoreactivity near the lesion (L) Asterisk marks the necrotic zone. Immediately below there is a zone (double asterisk) where vessels are devoid of immunoreactivity, although laminin immunostaining visualizes them (see above, panel **b**). Apart from this territory the vasculature is intensely labeled. **e.** The pattern visualized by α1-dystrobrevin immunoreactivity is similar to that of ß-dystroglycan (a parallel section is shown in panel **d**). **f.** Laminin immunostaining of the vessel shown on the left side of panel **b** (double labeling). L refers to lesion. Note that the vascular laminin immunostaining in the necrotic tissue is more intense (arrowhead) than in the underlying zone (double arrowhead). This distribution is the inverse of the pattern of utrophin immunostaining (see the right side of panel **g**). Arrow points to the outer (glial) basal lamina getting separated from the vascular one. **g.** Utrophin immunostaning. L refers to lesion. Labeled vessels (double arrowheads) appear at first at POD 7. Vascular labeling is less intense (arrowheads) in the necrotic tissue (asterisk); than in the underlying zone (arrowheads), i.e. inversely to that of laminin (see panel **f**). Scale bars: a, c, 250 μm; b, 120 μm; d, e, 60 μm; f, g, 50 μm; inset in c, 15 μm.

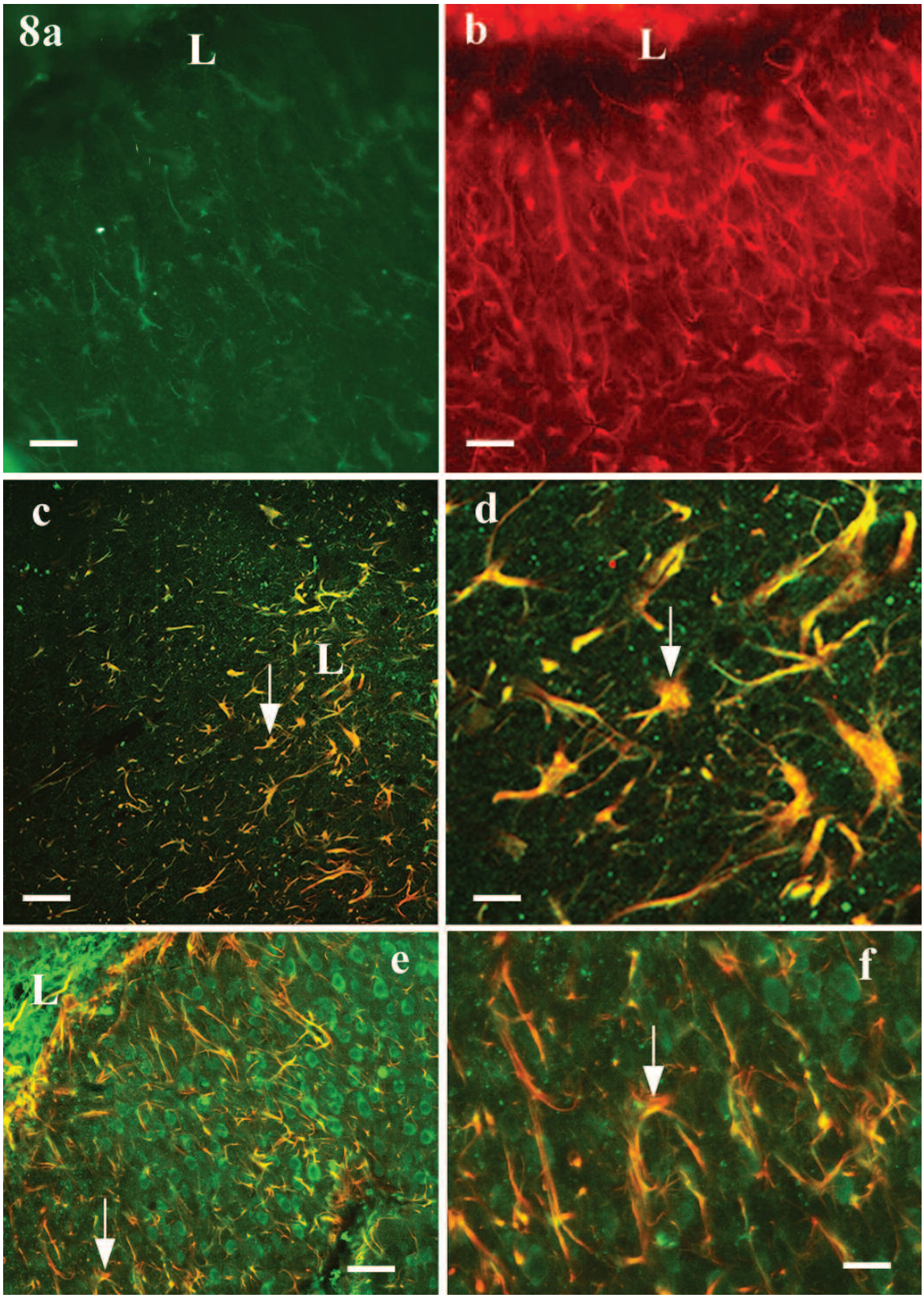

Fig. 8. α1-syntrophin colocalizes with GFAP. **a and b.** α1-syntrophin immunoreactivity **(a)** marks astrocyte-like cells at a cryogenic lesion (L) similar to the GFAP labeled ones **(b)** POD 14. **c and d.** Co-localization of GFAP and α1-syntrophin in astrocytes around a stab wound, POD 14, double labeling, confocal microscopy. Yellow and brownish colors refer to co-localization, green spots represent neurons. **e and f.** Co-localization of GFAP and α1-syntrophin at a cryogenic lesion (L), double labeling, confocal microscopy. For other explanations see panels **c and d.** Scale bars: a, b, 30 μm; c, e, 40 μm; d, f, 10 μm.

α1-syntrophin-immunopositve ones. Vascular immunopositivity underwent no conspicuous changes.

The α1-syntrophin immunopositivity of astrocytes disappeared during the 3rd week (Fig. 6c-f) when utrophin immunopositivity still persisted in the vessels, and ß-dystroglycan immunopositivity re-appeared. Most interestingly, the last α1-syntrophin immunostained astrocytes were found within the areas where ß-dystroglycan immunopositivity had not re-appeared yet.

Following cryogenic lesion: phenomena like above (Figs. 7 and 8)

Preliminary experiments suggested that the optimal duration of the freezing was 20 sec. In this case the lesions were quite large and similarly sized. They were lens-like (i.e deeper in the center), with a diameter approximately 1 mm. (Fig. 7a,c). Cryogenic lesion provoked an intense glial reaction which extended over the whole cortex (Fig. 7c). Altered laminin, ß-dystroglycan and α1-dystrobrevin immunoreactivities were observed already at POD 2, and became maximal between POD 4 and POD 7.

Laminin appeared within the territory of the lesion and even around it, although less intensely (Fig. 7a,b). Immunolabeled vessels were found mainly in the necrotic zone. The GFAP-immunopositive glial reaction was found most intensely in the zone devoid of ß-dystroglycan- and 1-dystrobrevin immunopositivities (Fig. 7c).

The immunopositivities to ß-dystroglycan and α1-dystrobrevin disappeared from the necrotic tissue as well as from the underlying zone (Fig. 7d,e). This zone was also penetrated by laminin-immunopositive vessels (Fig. 7a,b), some of them extended even beyond this zone into the territory of subsisting ß-dystroglycan and α1-dystrobrevin-immunopositive vessels.

Utrophin immunoreactivity appeared in the vessels at POD 7, at first in vessels turned formerly immunopositive to laminin adjacent to the necrotic zone. The number of utrophin-immunopositive vessels, however, increased during the second week (Fig. 7g), therefore they surpassed in number the laminin-positive ones, and occurred without laminin, too. In the double-labeled vessels it was clearly seen that the segments intruding into the necrotic zone were intensely immunoreactive to laminin but hardly immunoreactive to utrophin. In those parts which were embedded in the underlying brain substance the intensities were found to be quite the opposite (Fig. 7f,g). It is to be noted that in Fig. 7f it is clearly visible that the basal lamina splits into two layers. The outer, funnel-like layer probably belongs to the surrounding glia, whereas the inner layer represents the proper basal lamina of the endothelium.

α1-syntrophin immunoreactivity appeared temporarily in reactive astrocytes (Fig. 8a,b). Its co-localization with GFAP has been proved by fluorescent double labeling evaluated by confocal laser scanning microscopy (Fig. 8e,f), similarly to stab wounds (Fig. 8c,d). No other immunopositivities were observed in astrocytes. All of these alterations regressed by POD 21, and disappeared almost completely by POD 28, except as a remnant of the glial reaction. The results are summarized in Table 3.

The immunoreactivities of the same substance are compared at different postoperative days. Intensities were estimated by the sensitivity of the photoapparatus (see Methods).

Western blot results (Fig. 9)

In order to clarify whether the altered α1-dystrobrevin and α1-syntrophin immunoreactivities could be attributed to a change of the levels of these proteins or to other factors, we assessed their levels by semiquantitative Western blot analysis (Fig. 9) which

Table 3. Summary on the changes of the immunoreactivities investigated in this study.

	POD 2	POD 4	POD 7	POD 14	POD 21	POD 28
laminin	+	+	+	+/+-	+-	-
ß-dystroglycan	-	-	-	+-	+	+
α1-dystrobrevin	-	-	-	+-	+/+-	+
α1-syntrophin	+-	+-	+	++	+-/-	-
utrophin	-	-	+-	+	++	+-
GFAP	+-	+	++	++	+	+-

++: very intense; +: intense; +-: weak and/or not constant; -: missing.

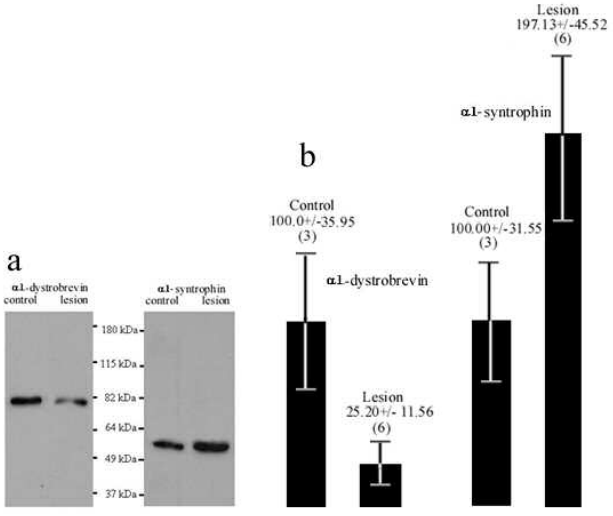

Fig. 9. Western blot analysis of post-lesion α1-syntrophin and α1-dystrobrevin levels. **a.** Representative blots of individual samples. **b.** Integrated densities (cf. Materials and Methods) indicative of protein levels are shown. Data were calculated from Western blots of at least 3 lesioned tissue samples, originating from distinct animals. Integrated densities of control samples were considered as 100%. Average and ± standard deviation values are shown, following the Student-test $p<0.05$.

indicated significantly lower α1-dystrobrevin and higher α1-syntrophin levels in the tissue samples taken from cryogenic-lesioned brains than from the control ones.

Discussion

The results presented here are in accordance with previous data on the immunoreactivities observed in the intact brain, as well as on the post-lesion alterations of laminin and ß-dystroglycan. Furthermore, we provide new data on the post-lesion behavior of α1-syntrophin, α1-dystrobrevin and utrophin. When comparing the characteristics of two different lesions, stab wound and cryogenic lesions, we concluded that they resulted in similar immunohistochemical consequences.

Laminin and DGC in the intact adult rat brain

The results obtained in intact animals were in general in good agreement with the data published in the literature and with our previous experience. Laminin was not detectable by immunohistochemistry in the vessels embedded in the brain substance, except the circumventricular organs, in accordance with several previous obsevations (Shigematsu et al., 1989b; Zhou, 1990; Krum et al., 1991), including ours (Szabó and Kálmán, 2008). Since in unfixed cryostat sections vessels were immunoreactive to laminin (Eriksdotter-Nilsson et al., 1986), it was suggested that it was the fixation which inhibited the immunoreactivity (Jucker et al., 1992). Nevertheless, immunoreactivity of the extracerebral vessels and those in the circumventricular organs do not support this idea. According to Krum et al. (1991), it is the fusion during development of the glial and vascular basal laminae (Bär and Wolff, 1972; Marin-Padilla, 1985; del Zoppo and Hallenbeck, 2000; Hallmann et al., 2005) into a so-called 'composite' basal lamina (Sixt et al., 2001) which covers ('hides') the epitopes responsible for immunoreactivity and makes them unavailable for immunohistochemical detection. Fixation enhances this effect whereas freezing (e.g. by ice crystals) eliminates it. The fusion does not occur in the circumventricular organs (Krum et al., 1991), which have no blood-brain barrier (the subcommissural organ represents an exception). For a more detailed discussion see (Szabó and Kálmán, 2004, 2008). Laminin immunopositivity of certain neurons (see e.g. Fig. 1a) has been already mentioned by several authors (Yamamoto et al., 1988; Hagg et al., 1989; Zhou, 1990; Jucker et al., 1992; Powell and Kleinman, 1997), although its role is not clear yet. Immunoreactivities of cerebral vessels and meningeal glia limitans to ß-dystroglycan are in accordance with the findings of Tian et al. (1996), Uchino et al. (1996), Zaccaria et al. (2001), Moore et al. (2002), Szabó and Kálmán (2008).

Brain vessels were also visualized by immunohistochemical reaction to α1-dystrobrevin, whereas ß1-dystrobrevin was found in neurons (Ueda et al., 1995; Blake et al., 1999). Immunoreactivity of α1-syntrophin was also found along the brain vessels (Haenggi et al., 2004; Ambrosini et al., 2008) as well as in neurons (Blake et al., 1999). Neither α1-dystrobrevin nor ß-dystroglycan nor α1-syntrophin was reported to be present in the meningeal vessels, in accordance with our observations.

Utrophin was found in blood vessels, either meningeal or cerebral, by *in situ* hybridization or by immunohistochemistry in cryostat sections (Ueda et al., 1995; Knuesel et al., 2000; Haenggi et al., 2004) or after fixation by perfusion (Knuesel et al., 2000). Although Khurana et al. (1992) reported its glial localization, recent opinion is that glial end-feet lack utrophin (Culligan and Ohlendieck, 2002; Haenggi and Fritschy, 2006; Wolburg et al., 2009). Since ß-dystroglycan occurs in the glial end-feet, but seems to be absent from the endothel (Tian et al., 1996; Hallmann et al., 2005; Haenggi and Fritschy, 2006) utrophin is probably bound to the cell membrane by another factor (Haenggi and Fritschy, 2006). Our observation that the circumventricular organs - e.g. subfornical organ, area postrema (but not the subcommissural organ, which, in contrast to the others, has blood–brain barrier), display vascular immunoreactivity to utrophin (like to laminin) seems to be a novelty.

Post-lesion phenomena: laminin and ß-dystroglycan:

As was demonstrated in several publications (Sosale et al., 1988; Shigematsu et al., 1989a,b; Krum et al., 1991; Sixt et al., 2001) including ours (Szabó and Kálmán, 2004, 2008) after lesions laminin became detectable by immunohistochemical reactions.

ß-dystroglycan immunostaining markedly decreased or was totally absent following focal ischemia (Milner et al., 2008) and in experimental autoimmune encephalomyelitis (Agrawal et al., 2006). Stab wounds resulted in a temporary lack of ß-dystroglycan immunopositivity in the vessels adjacent to the lesion (Szabó and Kálmán, 2008).

We demonstrated that laminin immunopositivity appeared mainly in those vessels which lost their ß-dystroglycan immunoreactivity, and *vice versa*, although there were double-labeled vessels as well. The fact that a major part of ß-dystroglycan-immunonegative vessels was revealed by immunostaining to laminin proved that a lack of ß-dystroglycan immunostaining doesn't indicate a lack of vessels. Both phenomena (i.e. ß-dystroglycan negativity and laminin positivity) can be regarded as indirect signs of gliovascular decoupling, and their disappearance may refer to restitution (re-coupling). To explain these phenomena we accept the opinions of Krum et al. (1991) and Milner et al. (2008).

After lesions, the astrocytic end-feet 'decouple' (detach) from the vessels and a substantial expansion of perivascular spaces becomes evident (Jaeger and Blight, 1997). Similar observations were published by Sixt et al. (2001) in inflammations. The post-lesion immunopositivity of cerebral vessels to laminin can be explained

by the post-lesion separation of glial and vascular basal laminae, and/or by the appearance of newly formed vessels in which the fusion of these basal laminae hasn't happened yet (Krum et al., 1991; Sixt et al., 2001). In both cases the laminin epitopes otherwise covered by the fusion of basal laminae, can become temporarily 'uncovered'. It is to be noted that besides laminin, nidogen (a basal lamina component which also binds to ß-dystroglycan) has also been reported to show diminished immunoreactivity due to altered epitope availability (Ae Seo et al., 2007).

Decreased ß-dystroglycan immunoreactivity can be attributed to the cleavage of ß-dystroglycan by matrix metalloproteinases (MMPs), as the experiments of Milner et al. (2008) suggest. MMPs -2 and -9 are able to remove that fragment of ß-dystroglycan, which connects it to α-dystroglycan, and thereby to laminin (Yamada et al., 2001; Zhong et al., 2006). It results in the decoupling of the gliovascular connections. Several data show that the activities of MMPs increase following cerebral lesions, e.g. cerebral ischemia (stroke model), trauma, or inflammation (Asahi et al., 2000; Chang et al., 2003; Fukuda et al., 2004; Yong, 2005; del Zoppo et al., 2007; Milner et al., 2008). MMP (collagenase) activity also promotes the immunohistochemical detectability of cerebrovascular laminin (Mauro et al., 1984; Krum et al., 1991). Actually, MMP activity can be one of the mechanisms of gliovascular decoupling mentioned in the previous paragraph (Wagner et al., 1997; del Zoppo and Milner, 2006). Another possible explanation is that the glial end-feet surrounding the newly formed vessels of revascularization don't yet express dystroglycan. However, Western blot studies of Milner et al. (2008) demonstrated a decrease in ß-dystroglycan level, which supports the former possibility. As our double labeled studies demonstrated, during vascular reparation ß-dystroglycan immunopositivity re-appears before that of laminin disappears. Their final convergence may refer to the ongoing vascular regeneration, the restitution of the gliovascular connections, and when these take place the laminin immunoreactivity disappears.

α1-dystrobrevin

Similarly to laminin, α-dystrobrevin immunoreactivity changed in concert with ß-dystroglycan immunoreactivity. However, whereas in the case of the transmembrane ß-dystroglycan the removal of its extracellular part by MMP-9 might provide an explanation, this explanation cannot be applied for α1-dystrobrevin. It is an intracellular peripheric protein connected to the intracellular part of ß-dystroglycan via dystrophin (Ueda et al., 1995; Amiry-Moghaddam et al., 2004). Therefore the correlation between their disappearance probably demands a more elaborated molecular mechanism e.g. the disintegration of the DGC as a consequence of the cleavage of ß-dystroglycan. Disintegration might expose α1-dystrobrevin to intracellular proteolytic degradation as suggested by the decreased protein level shown by Western blot analysis. It is to be noted that the correlation between the immunoreactivities of ß-dystroglycan and α1-dystrobrevin is not strict, because during repair (revascularization) the re-appearance of ß-dystroglycan immunoreactivity precedes that of α1-dystrobrevin. This might be attributed to a delay in its synthesis, and/or to the necessity of the re-establishment of the dystroglycan-dystrophin connection before the binding of α1-dystrobrevin.

Utrophin

Its 'behavior' was similar to that of laminin with which it frequently seemed even to co-localize. This co-localization, however, was not strict and the time-courses of the *post-lesion* appearance and disappearance of the two proteins were somewhat different. Utrophin immunohistochemistry detects numerous vessels in cryostat sectioned, unfixed, intact brain tissue (see Ueda et al., 1995; Knuesel et al., 2000; Haenggi et al., 2004 and our own unpublished observation). This fact renders the role of epitope hiding plausible, similarly to the cases of laminin and nidogen. Similarly to laminin, utrophin is also detectable in the area of the Virchow-Robin spaces and in those circumventricular organs where the blood-brain barrier is leaky and there is a space around the vessels, e.g. in the subfornical organ. Therefore the immunohistochemical detectability of utrophin seems to be in correlation with a space - maybe only in the molecular dimension - around the vessels, as is suggested for laminin (Krum et al., 1991). However, utrophin being positioned intracellularly, a more elaborated molecular mechanism is to be assumed to explain how structural changes of the basal lamina affect this protein.

Since in frozen (cryostat) sections of intact brain utrophin was immunoreactive, it proves that - like with laminin - its increased level is not an essential condition of the appearance of immunoreactivity in the brain vessels following lesions. It is to be mentioned, however, that in the meantime our colleagues studying another (ischemic) model estimated by Western blot an increased level of utrophin but not laminin (Wappler et al., 2011).

We suppose that as the detectability of laminin is in correlation with the destruction of the basal lamina and the dissolution of the gliovascular connections, the appearance of utrophin immunoreactivity is a sign of restitution. The fact that utrophin is not detectable in the territory of the destroyed, necrotic brain tissue, in contrast to laminin, indicates that utrophin immunoreactivity manifests only when the (endothelial) cells have not yet been destroyed completely.

Taking into account that utrophin is vascularly localized (Knuesel et al., 2000; Culligan and Ohlendieck, 2002; Haenggi et al., 2004; Haenggi and Fritschy, 2006; Wolburg et al., 2009), while the other DGC components investigated here are found in the glial cells, it is clear that the changes in utrophin

immunoreactivity do not correlate with those of the other DGC components studied. Utrophin is supposed to accompany ß2-syntrophin and ß1-dystrobrevin (Culligan and Ohlendieck, 2002; Haenggi and Fritschy, 2006).

α1-dystrobrevin immunopositivity re-appeared along the utrophin-positive vessels in a later phase of *post-lesion* reaction. We could not perform double-labeling studies of ß-dystroglycan and utrophin, as both antibodies were raised in mouse. However, we observed that: a) the re-appearance of ß-dystroglycan preceded both the re-appearance of α1-dystrobrevin and the disappearance of laminin, b) utrophin was still detected together with laminin and α1-dystrobrevin. Therefore we may suppose that the re-appearance of ß-dystroglycan immunopositivity also precedes the disappearance of utrophin.

α1-syntrophin

Following lesions, α1-syntrophin appeared in the reactive astrocytes. Western blot data showed a post-lesion increase of the protein level. Therefore we suggest that *post-lesion* glial reaction involves the elevated expression of α1-syntrophin. We might suppose that this step represents the preparation for the re-organization of the system of aquaporins and other channel and receptor proteins. Syntrophins are regarded as 'scaffolds' of DGC (Bragg et al., 2006). It is to be noted that no other proteins investigated here emerged in reactive astrocytes (except for, of course, GFAP). In our earlier studies (Szabó et al., 2004) in reactive astrocytes we detected the appearance of the spliced variant of the 71kD dystrophin isoform (Dp71f) using the antibody 5f3 produced by Mornet (Fabbrizio et al., 1994). Nevertheless, both the time courses and the areas of α1-syntrophin and GFAP expressions are different. The α1-syntrophin immunoreactivity developed later, in a more confined area, and regressed earlier than that of GFAP in the reactive astrocytes (for the latter one see also Bignami and Dahl, 1976; Berry et al., 1983; Mathewson and Berry, 1984; Hozumi et al., 1990). Further studies are clearly needed to reveal its roles in the reactive astrocytes.

Conclusions

This report describes the effects of two different cortical lesions – cryogenic and stab wound – on the immunoreactivities of the members of DGC and laminin. The phenomena were similar in both lesions. We suppose that similar alterations follow other cerebral injuries. The variations of immunoreactivities may reflect changes in the steric structure and/or interconnection of the DGC components. These changes are supposed to be suitable to characterize the stages of *post-lesion* vascular reactions, damage and repair, and help to monitor their progress, and provide – although indirectly - a look at the cellular and molecular events taking place.

Acknowledgements. This study was supported by the Hungarian Science Foundation, grant number: OTKA 2006/K 60930. The participations of the authors: M. Kálmán (senior): team leader, experimental design, evaluations, design of the manuscript. J. Mahalek and S. Sadeghian (undergraduate students): cryogenic lesions and immunohistochemistry, I. Adorján, Z. Bagyura and K. Pócsai (PhD students): stab wounds and immunohistochemistry, A. Adorján (PhD student): Western blot studies. Helpful comments of dr. V. Jancsik (Dept. of Anatomy, Szt István University), methodical advices of T. Balázsa and the technical assistance of S. Deák and Z. A. Őz are highly appreciated (Dept. of Anatomy, Histology and Embryology, Semmelweis University).

References

Abbott N.J. (2002). Astrocyte-endothelial interactions and blood-brain barrier permeability. J. Anat. 200, 629-638.

Ae Seo I., Kyoung Lee H., Mi Park Y., Jin Ahn K. and Tae Park H. (2007). Acute changes of nidogen immunoreactivity in the basal lamina of the spinal cord vessels following dorsal hemisection without correlative changes of nidogen gene expression. Acta Histochem. 109, 446-453.

Agrawal S., Anderson P., Durbeej M., van Rooijen N., Ivars F., Opdenakker G. and Sorokin L.M. (2006). Dystroglycan is selectively cleaved at the parenchymal basement membrane at sites of leukocyte extravasation in experimental autoimmune encephalomyelitis. J. Exp. Med. 203, 1007-1019.

Ambrosini E., Serafini B., Lanciotti A., Tosini F., Scialpi F., Psaila R., Raggi C., Di Girolamo F., Petrucci T.C. and Aloisi F. (2008). Biochemical characterization of MLC1 protein in astrocytes and its association with the dystrophin-glycoprotein complex. Mol. Cell Neurosci. 37, 480-493.

Amiry-Moghaddam M., Frydenlund D.S. and Ottersen O.P. (2004). Anchoring of aquaporin-4 in brain: molecular mechanisms and implications for the physiology and pathophysiology of water transport. Neuroscience 129, 999-1010.

Asahi M., Asahi K., Jung C., del Zoppo G.J., Fini M.E. and Lo E.H. (2000). Role for matrix metalloproteinase 9 after focal cerebral ischemia: effects of gene knockout and enzyme inhibition with BB-94. J. Cereb. Blood Flow Metab. 20, 1681-1689.

Bär T.H. and Wolff J.R. (1972). The formation of capillary basement membranes during internal vascularization of the rat's cerebral cortex. Z. Zellforsch. 133, 231-248.

Bernstein J.J., Getz R., Jefferson M. and Kelemen M. (1985). Astrocytes secrete basal lamina after hemisection of rat spinal cord. Brain Res. 327, 135-141.

Berry M., Maxwell W.I., Logan A., Mathewson A., McConnell P., Ashhurst D.E. and Thomas G.H. (1983). Deposition of scar tissue in the central nervous system. Acta Neurochir. Suppl. 32, 31-53.

Bignami A. and Dahl D. (1976). The astroglial response to stabbing. Immunofluorescence studies with antibodies to astrocyte-specific protein (GFAP) in mammalian and submammalian vertebrates. Neuropathol. Appl. Neuro. 2, 99-110.

Blake D.J., Hawkes R., Benson M.A. and Beesley P.W. (1999). Different dystrophin-like complexes are expressed in neurons and glia. J. Cell Biol. 147, 645-658.

Bragg A.D., Amiry-Moghaddam M., Ottersen O.P., Adams M.E. and

Froehner S.C. (2006). Assembly of a perivascular astrocyte protein scaffold at the mammalian blood–brain barrier is dependent on -syntrophin. Glia 53, 879–890.

Chang D.I., Hosomi N., Lucero J., Heo J.H., Abumiya T., Mazar A.P. and Del Zoppo G.J. (2003). Activation systems for latent matrix metalloproteinase-2 are upregulated immediately after focal cerebral ischemia. J. Cereb. Blood Flow Metab. 23, 1408-1419.

Chiu A.Z., Espinosa de los Monteros A., Cole R.A., Loera S. and J de Vellis. (1991). Laminin and s-laminin are produced and released by astrocytes, Schwann-cells and schwannomas. Glia 4, 11-24.

Culligan K. and Ohlendieck K. (2002). Diversity of the brain dystrophin-glycoprotein complex. J. Biomed. Biotechnol. 2, 31–36.

del Zoppo G.J. and Hallenbeck J.M. (2000). Advances in the vascular pathophysiology of ischemic stroke. Thromb. Res. 98, 73-81.

del Zoppo G.J. and Milner R. (2006). Integrin-matrix interactions in cerebral microvasculature. Atheroscler. Thromb. Vascul. Biol. 26, 1966-1975.

del Zoppo G.J., Milner R., Mabuchi T., Hung S., Wang X. and Koziol J.A. (2006). Vascular matrix adhesion and the blood-brain barrier. Biochem. Soc. Trans. 34, 1261-1266.

del Zoppo G.J., Milner R., Mabuchi T., Hung S., Wang X., Berg G.I. and Koziol J.A. (2007). Microglial activation and matrix protease generation during fical cerebral ischemia. Stroke 38, 646-651.

Durbeej M., Henry M.D. and Campbell K.P. (1998). Dystroglycan in development and disease. Curr. Opin. Cell Biol. 10, 594-601.

Eriksdotter-Nilsson M., Björklund H. and Olson L. (1986). Laminin immunohistochemistry is a simple method to visualize and quantitate vascular structures in the mammalian brain. J. Neurosci. Meth. 17, 275-286.

Fabbrizio E., Nudel U., Hugon G., Robert A., Pons F. and Mornet D. (1994). Characterization and localization of a 77 kDa protein related to the dystrophin gene family. Biochem. J. 299, 359-365.

Fukuda S., Fini C.A., Mebuchi T., Koziol J.A., Eggleston L.L. and del Zoppo G.J. (2004). Focal cerebral ischaemia induces active proteases that degrade microvascular matrix. Stroke 35, 998-1004.

Gorecki D.C., Monaco A.P., Derry J.M.J., Walker A.P., Barnard E.A. and Barnard P.J. (1992). Expression of four alternative dystrophin transcripts in brain regions regulated by different promoters. Hum. Mol. Genet. 1, 505-510.

Guadagno E. and Moukhles K. (2004). Laminin-induced aggregation of the inwardly rectifying potassium channel, Kir4.1, and the water permeable channel, AQP4 via a dystroglycan-containing complex in astrocytes. Glia 47, 138-149.

Haenggi T. and Fritschy J.M. (2006). Role of dystrophin and utrophin for assembly and function of the dystrophin glycoprotein complex in non-muscle tissue. Cell Mol. Life Sci. 63, 1614-1631.

Haenggi T., Soontornmalai A., Schaub M.C. and Fritsch J-M. (2004). The role of utrophin and Dp71 for assembly of different dystrophin-associated protein complexes (DPCs) in the choroid plexus and microvasculature of the brain. Neuroscience 129, 403-413.

Hagg T., Muir D., Engvall E., Varon S. and Manthorpe M. (1989). Laminin-like antigen in rat CNS neurons: distribution and changes upon brain injury and nerve growth factor tratment. Neuron 3, 721-732.

Hallmann R., Horn N., Selg M., Wendler O., Pausch F. and Sorokin L.M. (2005). Expression and function of laminins in the embryonic and mature vasculature. Physiol. Rev. 85, 979-1000.

Henry M.D. and Campbell K.P. (1996a). Dystroglycan: an extracellular matrix receptor linked to cytoskeleton. Curr. Opin. Cell Biol. 8, 625-631.

Henry M.D. and Campbell K.P. (1996b). Dystroglycan inside and out. Curr. Opin. Cell Biol. 11, 602-607.

Hozumi I., Chiu F.C. and Norton W.T. (1990). Biochemical and immunocytochemical changes in the glial fibrillary acidic protein after stab wounds. Brain. Res. 485, 235-324.

Ibraghimov-Beskrovnaya O., Ervasti J.M., Leveille C.J., Slaughter C.A., Sernett S.W. and Campbell K.P. (1992). Primary structure of dystrophin-associated glycoproteins linking dystrophin to the extracellular matrix. Nature 355, 696-702.

Jaeger C.B. and Blight A.R. (1997). Spinal cord compression injury in guinea pigs: structural changes of endothelium and its perivascular cell associations after blood-brain barrier breakdown and repair. Exper. Neur. 144, 381-399.

Jancsik V. and Hajós F. (1998). Differential distribution of dystrophin in postsynaptic densities of spine synapses. Neuroreport 9, 2249-2251.

Jancsik V. and Hajós F. (1999). The demonstration of immunoreactive dystrophin and its developmental expression in perivascular astrocytes. Brain Res. 831, 200-205.

Janzer R.C. and Raff M.C. (1987). Astrocytes induce blood-brain barrier properties in endothelial cells. Nature 325, 253-257.

Jucker M., Bialobok P., Hagg T. and Ingram D.K. (1992). Laminin immunohistochemistry in brain is dependent on method of tissue fixation. Brain Res. 586, 166-170.

Jucker M., Tian M. and Ingram D.K. (1996). Laminins in the adult and aged brain. Mol. Chem. Neuropath. 28, 209-218.

Khurana T.S., Watkins S.C. and Kunkel L.M. (1992). The subcellular distribution of chromosome 6-encoded dystrophin-related protein in the brain. J. Cell Biol .119, 357-366.

Knuesel I., Bornhauser B.C., Zuellig R.A., Heller F., Shaub M.C. and Fritschy J.M. (2000). Differential expression of utrophin and dystrophin in CNS neurons: an in situ hybridization and immunohistochemical study. J. Comp. Neurol. 422, 594-611.

Krum J.M., Mani N. and Rosenstein J.M. (2002). Angiogenic and astroglial responses to vascular endothelial growth factor administration in adult rat brain. Neuroscience 110, 589-604.

Krum J.M., More N.S. and Rosenstein J.M. (1991). Brain angiogenesis: variations in vascular basement membrane glycoprotein immunoreactivity. Exp. Neurol. 111, 151-165.

Laemmli U.K. (1970). Cleavage of structural proteins during the assembly of the head of bacteriophage T4. Nature 227, 680-685.

Lederfein D., Levy Z., Augier N., Mornet D., Morris G., Fuch O., Yaffe D. and Nudel U. (1992). A 71-kilodalton protein is a major product of Duchenne muscular dystrophin gene in brain and other nonmuscle tissues. Proc. Natl. Acad. Sci. USA 89, 5346-5350.

Lidov H.G.W. (1996). Dystrophin in the nervous system. Brain Pathol. 6, 63-77.

Liesi P., Kaakkola S., Dahl D. and Vaheri A. (1984). Laminin is induced in astrocytes of adult brain injury. EMBO J. 3, 683-686.

Lowry O.H., Rosebrough N.J., Farr A.L. and Randall R.J. (1951). Protein measurement with the Folin phenol reagent. J. Biol. Chem. 193, 265-275.

Marin-Padilla M. (1985). Early vascularization of the embryonic cerebral cortex: Golgi and electron microscopic studies. J. Comp. Neurol. 241, 237-249.

Mathewson A.J. and Berry M. (1984). Observations on the astrocytic response to a cerebral stab wound in adult rats. Brain Res. 327, 61-69.

Mauro A., Bertolotto A., Germano I., Giaccone G., Giordana M.T., Migheli A. and Schiffer D. (1984). Collagenase in the immunohistochemical demonstration of laminin, fibronectin and factor VIII/Rag. Histochemistry 80, 157-163.

Milner R., Hung S., Wamg X., Spatz M. and del Zoppo G.J. (2008). The rapid decrease in astrocyte-associated dystroglycan expression is protease dependent. J. Cereb. Blood Flow Metab. 28, 812-823.

Moore S.A., Saito F., Chen J., Michele D.E., Henry M.D., Messing A., Cohn R.D., Ross-Barta S.E., Westra S., Williamson R.A., Hoshi T. and Campbell K.P. (2002). Deletion of brain dystroglycan recapitulates aspects of congenital muscular dystrophy. Nature 418, 422-425.

Neely J.D., Amiry-Moghaddam M., Ottersen O.P., Froehner S.C., Agre P. and Adams M.E. (2001). Syntrophin-dependent expression and localization of aquaporin-4 water-channel protein. Proc. Natl. Acad. Sci. USA 98, 14108-14113.

Nico B., Frigeri A., Nicchia G.P., Corsi P., Ribatti D., Quondamatteo F., Herken R., Girolamo F., Marzullo A., Svelto M. and Roncali L. (2003). Severe alterations of endothelial and glial cells in the blood-brain barrier of dystrophic mdx mice. Glia 42, 235-251.

Nico B., Nicchia G.P., Frigeri A., Corsi P., Mangieri D., Ribatti D., Svelto M. and Roncali L. (2004). Altered blood-brain barrier development in dystrophic MDX mice. Neuroscience 125, 921-935.

Powell S. and Kleinman H.K. (1997). Neuronal laminins and their cellular receptors. Int. Biochem. Cell Biol. 29, 401-414.

Riseau W. and Wolburg H. (1990). Development of the blood-brain barrier. Trends Neurosci. 13, 174-178.

Shigematsu K., Kamo H., Akiguchi J., Kameyama M. and Kimura H. (1989a). Neovascularization of transplanted central nervous tissue suspensions: an immunohistochemical study with laminin. Neurosci. Lett. 99, 18-23.

Shigematsu K., Kamo H., Akiguchi J., Kimura J., Kameyama M. and Kimura H. (1989b). Neovascularization in kainic acid-induced lesions of rat striatum. An immunocytochemical study with laminin. Brain Res. 501, 215-222.

Sixt M., Engelhardt B., Pausch F., Hallman R., Wendler O. and Sorokin L.M. (2001). Endothelial cell laminin isoforms, laminin 8 and 10, play decisive roles in T cell recruiment across the blood-brain barrier in experimental autoimmun encephalomyelitis. J. Cell Biol. 153, 933-945.

Smalheiser N.R. and Kim E. (1995). Purification of cranin, a laminin binding membrane protein. Identity with dystroglycan and reassessment of its carbohydrate moieties. J. Biol. Chem. 270, 15425-15433.

Sosale A., Robson J.A. and Stelzner D.J. (1988). Laminin distribution during corticospinal tract development and after spinal cord injury. Exp. Neurol. 102, 14-22.

Szabó A. and Kálmán M. (2004). Disappearance of the post-lesional laminin immunopositivity of brain vessels is parallel with the formation of gliovascular junctions and common basal lamina. A double-labeling immunohistochemical study. Neuropath. Appl. Neurobiol. 30, 169- 170.

Szabó A. and Kálmán M. (2008). Post traumatic lesion absence of ß-dystroglycan immunopositivity in brain vessels coincides with the glial reaction and the immunoreactivity of vascular laminin. Curr. Neurovasc. Res. 5, 206-213.

Szabó A., Jancsik V., Mornet D. and Kálmán M. (2004). Immunofluorescence mapping of dystrophin in rat brain: astrocytes contain the splice variant Dp71f but confined to subpopulations. Anat. Embryol. 208, 463-477.

Tao-Cheng J.H., Nagy Z. and Brightman M.W. (1987). Tight junctions of brain endothelium in vitro are enhanced by astroglia. J. Neurosci. 7, 3293-3299.

Tian M., Jacobson C., Gee S.H., Campbell K.P., Carbonetto S. and Jucker M. (1996). Dystroglycan in the cerebellum is a laminin ·2-chain binding protein at the glial-vascular interface and is expressed in Purkinje cells. Eur. J. Neurosci. 8, 2739-2747.

Uchino M., Hara A., Mizuno Y., Fujiki M., Nakamura T., Tokunaga M., Hirano T., Yamashita T., Uyama E., Ando Y., Mita S. and Ando M. (1996). Distribution of dystrophin and dystrophin-associated protein 43DAG (beta-dystroglycan) in the central nervous system of normal controls and patients with Duchenne muscular dystrophy. Intern. Med. 35, 189-94.

Ueda H., Baba T., Terada N., Kato Y., Fujii Y., Takayama I., Mei X. and Ohno S. (1995). Immunolocalization of dystrobrevin in the astrocytic endfeet and endothelial cells in the rat cerebellum. Neurosci. Lett. 283, 121-124.

Wagner S., Tagaya M., Koziol J.A., Quaranta V. and del Zoppo G.J. (1997). Rapid disruption of an astrocyte interaction with the extracellular matrix mediated by integrin ·6,4 during focal cerebral ischemia/perfusion. Stroke 28, 858-65.

Wappler E.A., Adorján I., Gál A., Galgóczy P., Bindics K. and Nagy Z. Dynamics of dystroglycan complex proteins and laminin changes due to angiogenesis in rat cerebral hypoperfusion. Microvasc. Res. 81, 153-159.

Warth A., Mittelbronn M. and Wolburg H. (2004). Redistribution of aquaporin-4 in human glioblastoma correlates with loss of agrin immunoreactivity from brain capillary basal laminae. Acta. Neuropath. 107, 311-318.

Wolburg H., Noell S., Mack A., Wolburg-Buchholz K. and Fallier-Becker P. (2009). Brain endothelial cells and the glio-vascular complex. Cell Tissue Res. 335, 75-96.

Yamada H., Saito F., Fukuta-Ohi K., Zhong D., Hase A., Arai K., Okuyama A., Maekawa R., Shimizu T. and Matsumura K. (2001). Processing of ß-dystroglycan by matrix metalloproteinase disrupts the link between the extracellular matrix and cell membrane via the dystroglycan complex. Hum. Mol. Gen. 10, 1563-1569.

Yamamoto T., Iwasaki Y., Yamamoto H., Konno H. and Isemura M. (1988). Intraneuronal lamininlike molecule in the central nervous system: demonstration of its unique differential distribution. J. Neurol. Sci. 84, 1-13.

Yong V.W. (2005). Metalloproteinases:mediators of pathology and regeneration in the CNS. Nat. Rev. Neurosci. 6, 931-944.

Zaccaria M.L., Di Tommaso F., Brancaccio A., Paggi P. and Petrucci T.C. (2001). Dystroglycan distribution in adult mouse brain: a light and electron microscopic study. Neuroscience 104, 311-324.

Zhong D., Saito F., Saito Y., Nakamura A., Shimizu T. and Matsumura T. (2006). Characterization of the protease activity that cleaves the extracellular domain of ß-dystroglycan. Biochem. Biophys. Res. Comm. 345, 867-871.

Zhou F.C. (1990). Four patterns of laminin-immunoreactive structure in developing rat brain. Dev. Brain Res. 55, 191-201.

Accepted January 1, 2011